

# Chapter 5

## Spectral Filtering and Photonic Spectral Engineering

*From Discrete Dichroics to Integrated Photonic Solutions*

This chapter develops the **spectral component of the Measurement Operator  $\mathcal{M}$** . The fundamental task is separating excitation photons from NV fluorescence while preserving quantum state information encoded in subtle intensity variations. Proper design achieves: (1)  $> 10^6:1$  excitation rejection, (2)  $> 90\%$  phonon sideband collection, (3) minimal model-mismatch penalty  $\Gamma_{mm}^{\text{spectral}} > 0.95$ , and (4) wavelength-division multiplexing for multi-physics QFI.

**QFI Pipeline Position:**  $S \xrightarrow{\mathcal{G}} F \xrightarrow{\mathcal{M}_{\text{spectral}}} D \xrightarrow{\mathcal{R}} \hat{S}$

### Abbreviated Terms

Term	Definition	Term	Definition
AOI	Angle of Incidence	AWG	Arrayed Waveguide Grating
FSR	Free Spectral Range	LCA	Longitudinal Chromatic Aberration
LP	Long-Pass	MRR	Micro-Ring Resonator
NV	Nitrogen-Vacancy	OD	Optical Density ( $OD = -\log_{10} T$ )
PBS	Polarization Beam Splitter	PIC	Photonic Integrated Circuit
PSB	Phonon Sideband	SBR	Signal-to-Background Ratio
SiN	Silicon Nitride	SP	Short-Pass
TE	Transverse Electric	TIR	Total Internal Reflection
TM	Transverse Magnetic	WDM	Wavelength Division Multiplexing
ZPL	Zero-Phonon Line	DOP	Degree of Polarization

Table 5.1: Abbreviated terms used in Chapter 5.

### Abstract

Spectral filtering in Quantum Field Imaging faces a fundamental challenge: achieving  $> 10^6:1$  excitation rejection while maximizing collection of the broad NV phonon sideband (637–800 nm). This chapter presents a comprehensive treatment spanning **two paradigms**: discrete thin-film optics and integrated photonic solutions.

We begin with thin-film interference theory and discrete dichroic design, establishing the classical approach that dominates current QFI implementations. The angle-of-incidence (AOI) induced blue shift of  $\approx 0.07\lambda_0$  ( $\sim 40$  nm at 580 nm edge) and cone-averaging effects in high-NA systems are quantified with explicit derivations linking physics parameters to the model-mismatch factor  $\Gamma_{mm}$ .

The chapter then introduces **photonic integrated spectral engineering**—a paradigm shift addressing discrete optics limitations through monolithic integration. Silicon nitride (SiN) platforms enable on-chip spectral filtering with key advantages, though we clarify that while AOI sensitivity is eliminated, waveguide dispersion and coupler spectral dependence introduce

new considerations requiring careful design.

We derive explicit relationships between filter specifications (layer count, thermal stability, channel isolation) and reconstruction fidelity  $\Gamma_{\text{inv}}$ , establishing that multi-physics WDM with  $>20$  dB channel isolation improves  $\Gamma_{\text{inv}}$  by 30–50% through condition number reduction. The chapter concludes with technology selection criteria, demonstrating integrated photonics becomes cost-effective above  $\sim 500$  production units.

## 5.1 Introduction: The Spectral Challenge in QFI

### 5.1.1 Why Spectral Filtering Matters for Quantum State Fidelity

Spectral filtering in QFI is not merely about separating excitation from emission—it is fundamentally about **preserving quantum information** encoded in subtle fluorescence variations during ODMR measurements. Any spectral imperfection manifests as noise that degrades the model-mismatch factor  $\Gamma_{\text{mm}}$ , directly impacting reconstruction fidelity  $\Gamma_{\text{inv}}$ .

The NV<sup>−</sup> center presents a unique spectral challenge:

- **Excitation:** 510–560 nm (optimal at 532 nm)
- **Zero-Phonon Line (ZPL):** 637 nm ( $\sim 3\%$  of emission)
- **Phonon Sideband (PSB):** 637–800 nm ( $\sim 97\%$  of emission)
- **Required rejection:**  $> 10^6:1$  at excitation wavelength
- **Required transmission:**  $> 90\%$  across PSB for photon budget

**Definition 5.1.1** (Optical Density). Optical Density (OD) quantifies blocking power on a logarithmic scale:

$$\text{OD} = -\log_{10} T \quad (5.1)$$

where  $T$  is the power transmission. Thus OD 6 corresponds to  $T = 10^{-6}$  or  $10^6:1$  rejection ratio.

#### Key Equation: Spectral Filtering Impact on $\Gamma_{\text{mm}}$

The model-mismatch penalty from spectral filtering errors is:

$$\Gamma_{\text{mm}}^{\text{spectral}} = \left(1 - \frac{\sigma_{\text{leak}}^2}{\sigma_{\text{signal}}^2}\right) \times \left(1 - \frac{\Delta\eta_{\text{collection}}}{\eta_{\text{nominal}}}\right) \quad (5.2)$$

where  $\sigma_{\text{leak}}$  is leakage-induced noise and  $\Delta\eta_{\text{collection}}$  is collection efficiency variation across the field.

### 5.1.2 The Two Paradigms: Discrete vs. Integrated

This chapter presents spectral filtering through two complementary paradigms:

Table 5.2: Paradigm comparison: discrete optics vs. photonic integration.

Aspect	Discrete Dichroics	Photonic Integration
Technology maturity	High (TRL 9)	Medium (TRL 5–7)
AOI sensitivity	Major challenge	Eliminated
Thermal stability	Passive ( $0.02 \text{ nm}/\text{°C}$ )	Active ( $<0.001 \text{ nm}/\text{°C}$ )
Waveguide dispersion	N/A	Requires management
Cost at 1 unit	\$500–2,000	\$10,000–50,000
Cost at 1,000 units	\$400–1,500	\$50–200
Multi-wavelength	Multiple filter sets	Integrated WDM
Polarization control	External components	On-chip PBS

### 5.1.3 Historical Development and Technology Trajectory

Table 5.3: Historical milestones in spectral filtering for quantum sensing.

Year	Milestone	Significance
1960s	Multilayer thin-film theory	Macleod, Thelen establish design methods
1990s	Dichroic filters for fluorescence	Standard in confocal microscopy
2008	First wide-field NV imaging	Demonstrated need for high OD filtering
2015	>OD6 edge filters commercial	Enabled practical NV-based sensing
2018	SiN photonics at visible wavelengths	Platform maturity for 532–800 nm
2020	On-chip NV integration demos	Proof of monolithic spectral control
2023	Integrated WDM for multi-physics	Simultaneous B/T/strain channels

### 5.1.4 Chapter Roadmap

1. **Sections 5.2–5.4:** Thin-film fundamentals and discrete dichroic design with quantitative derivations
2. **Sections 5.5–5.6:** Integrated photonic solutions and WDM for multi-physics, including dispersion management
3. **Sections 5.7–5.9:** Chromatic aberration, polarization, and thermal stability
4. **Sections 5.10–5.12:** SWOT analysis, risk mitigation, and worked examples with explicit  $\Gamma_{\text{inv}}$  connections

## 5.2 Thin-Film Interference Theory

### 5.2.1 Single-Layer Interference: First Principles

The reflectance of a thin film arises from interference between waves reflected at the two interfaces. For a film of refractive index  $n$  and thickness  $d$  on a substrate of index  $n_s$ , illuminated from medium  $n_0$  at angle  $\theta_0$ :

**Definition 5.2.1** (Optical Phase Thickness). The optical phase accumulated in a thin film is:

$$\delta = \frac{2\pi}{\lambda}nd \cos \theta \quad (5.3)$$

where  $\theta$  is the refraction angle in the film given by Snell's law:  $n_0 \sin \theta_0 = n \sin \theta$ .

The Fresnel reflection coefficients at each interface depend on polarization:

$$r_s = \frac{n_0 \cos \theta_0 - n \cos \theta}{n_0 \cos \theta_0 + n \cos \theta} \quad (5.4)$$

$$r_p = \frac{n \cos \theta_0 - n_0 \cos \theta}{n \cos \theta_0 + n_0 \cos \theta} \quad (5.5)$$

### 5.2.2 Characteristic Matrix Method

For multilayer stacks, the characteristic matrix method provides systematic analysis.

**Theorem 5.2.1** (Characteristic Matrix). *Each layer  $j$  with refractive index  $n_j$ , thickness  $d_j$ , and phase thickness  $\delta_j$  contributes a transfer matrix:*

$$M_j = \begin{pmatrix} \cos \delta_j & \frac{i \sin \delta_j}{\eta_j} \\ i \eta_j \sin \delta_j & \cos \delta_j \end{pmatrix} \quad (5.6)$$

where  $\eta_j = n_j \cos \theta_j$  (TE) or  $\eta_j = n_j / \cos \theta_j$  (TM).

The total system matrix for  $N$  layers is:

$$M_{\text{total}} = \prod_{j=1}^N M_j = \begin{pmatrix} m_{11} & m_{12} \\ m_{21} & m_{22} \end{pmatrix} \quad (5.7)$$

The reflectance and transmittance follow from:

$$r = \frac{\eta_0 m_{11} + \eta_0 \eta_s m_{12} - m_{21} - \eta_s m_{22}}{\eta_0 m_{11} + \eta_0 \eta_s m_{12} + m_{21} + \eta_s m_{22}}, \quad R = |r|^2 \quad (5.8)$$

### 5.2.3 High-Low Index Stack Design

The standard approach for high-OD edge filters uses alternating high-index ( $n_H$ ) and low-index ( $n_L$ ) quarter-wave layers.

**Proposition 5.2.1** (Quarter-Wave Stack Reflectance). *For  $N$  pairs of quarter-wave layers ( $n_H d_H = n_L d_L = \lambda_0/4$ ) at the design wavelength  $\lambda_0$ :*

$$R = \left( \frac{1 - (n_H/n_L)^{2N} (n_H^2/n_s)}{1 + (n_H/n_L)^{2N} (n_H^2/n_s)} \right)^2 \quad (5.9)$$

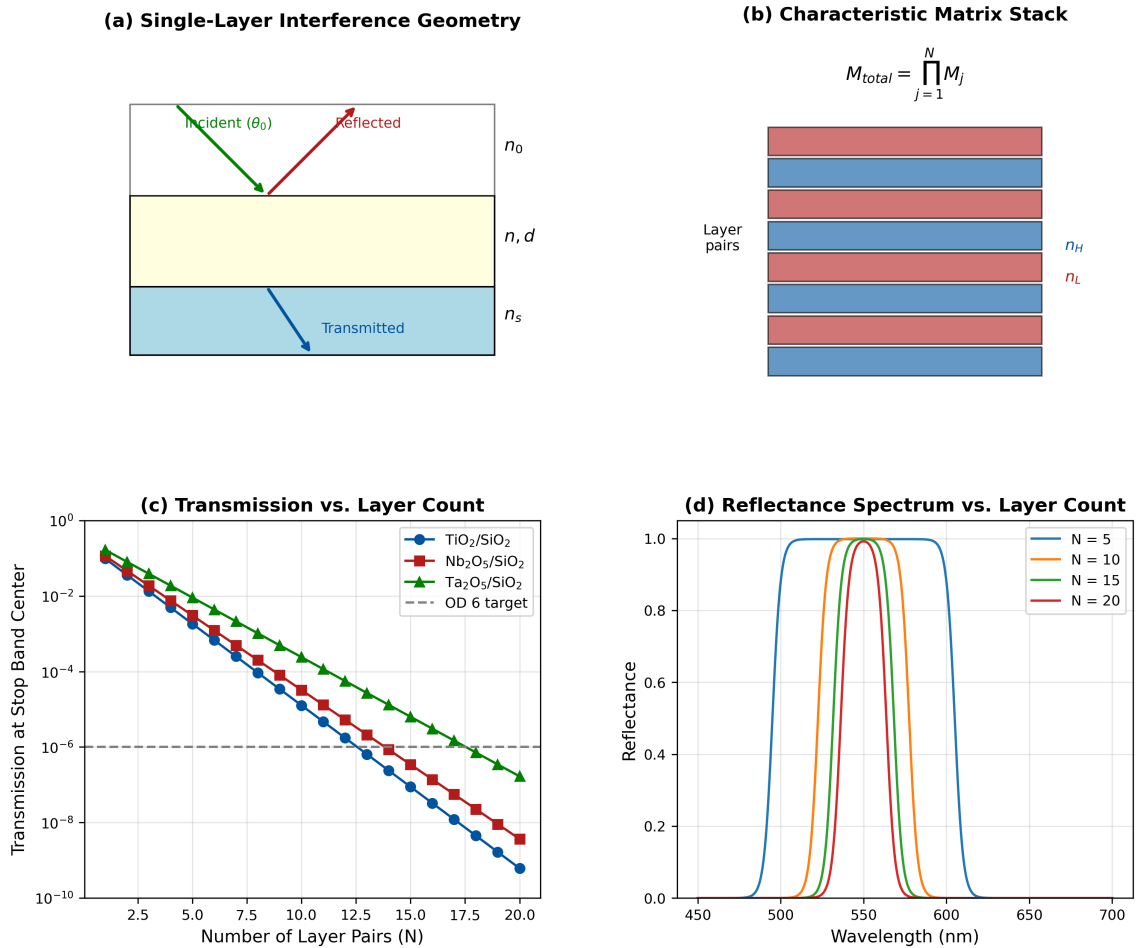


Figure 5.1: Thin-film interference fundamentals. (a) Single-layer interference geometry showing incident, reflected, and transmitted waves. (b) Characteristic matrix stack representation. (c) Quarter-wave stack reflectance vs. number of layer pairs for  $\text{TiO}_2/\text{SiO}_2$  ( $n_H = 2.4$ ,  $n_L = 1.46$ ). (d) Reflectance spectrum showing bandwidth vs. layer count.

### 5.3 NV Center Emission Spectrum Analysis

#### 5.3.1 Zero-Phonon Line and Phonon Sideband

The  $\text{NV}^-$  center emission spectrum consists of two distinct components:

**Definition 5.3.1** (NV Emission Components).

- **Zero-Phonon Line (ZPL):** Direct electronic transition at 637 nm, comprising  $\sim 3\%$  of total emission at room temperature
- **Phonon Sideband (PSB):** Phonon-assisted transitions spanning 637–800 nm, comprising  $\sim 97\%$  of emission

The Debye-Waller factor  $\alpha_{DW}$  quantifies ZPL fraction:

$$\alpha_{DW} = \frac{I_{ZPL}}{I_{\text{total}}} = \exp \left( -S \coth \frac{\hbar \omega_{\text{phonon}}}{2k_B T} \right) \quad (5.10)$$

where  $S \approx 3.7$  is the Huang-Rhys factor for NV centers.

### 5.3.2 Spectral Model for Filter Design

For filter design, we model the PSB as a sum of Gaussian components:

$$I_{\text{PSB}}(\lambda) = \sum_{k=1}^3 A_k \exp \left( -\frac{(\lambda - \lambda_k)^2}{2\sigma_k^2} \right) \quad (5.11)$$

Table 5.4: PSB spectral model parameters at room temperature.

Component	$\lambda_k$ (nm)	$\sigma_k$ (nm)	$A_k$ (rel.)
Near-PSB	665	15	0.35
Mid-PSB	700	25	0.45
Far-PSB	750	30	0.20

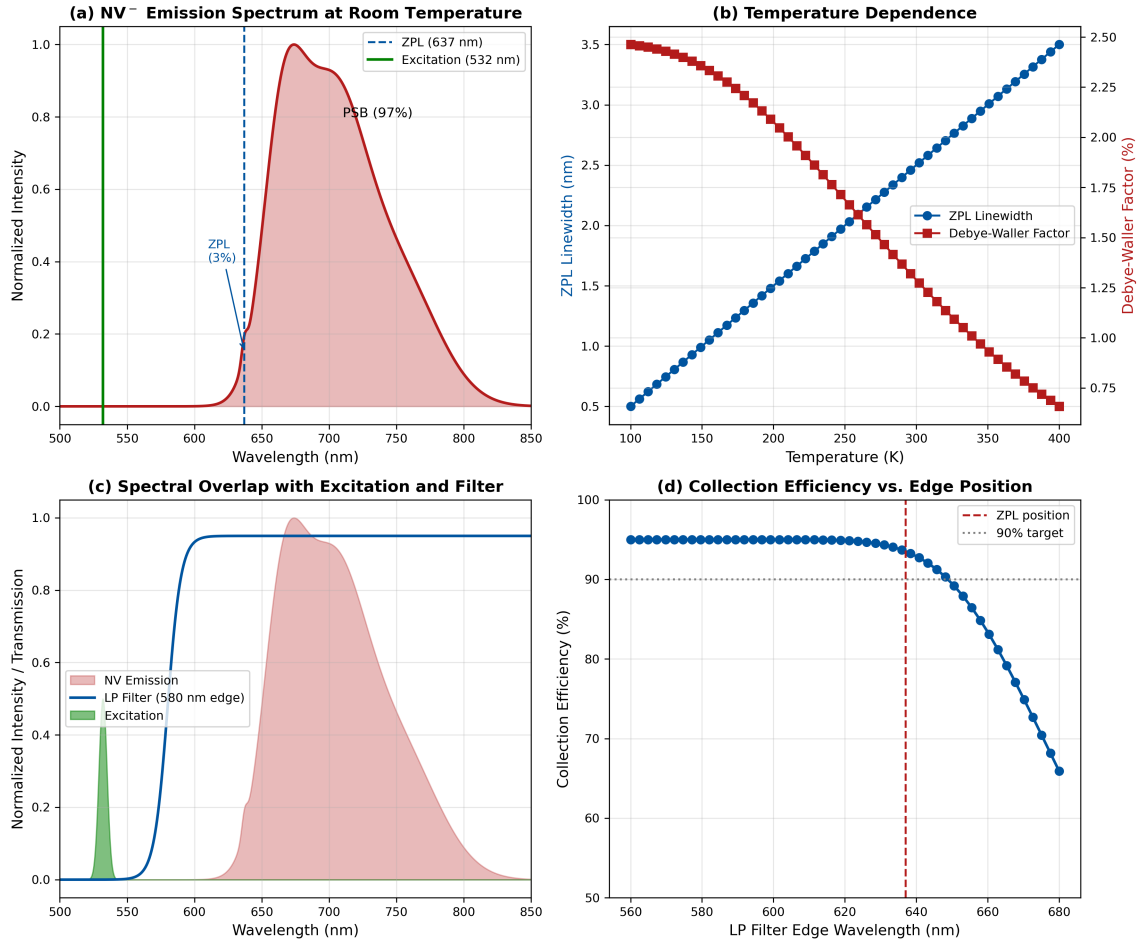


Figure 5.2: NV<sup>-</sup> center emission spectrum. (a) Complete emission spectrum showing ZPL at 637 nm and PSB extending to 800 nm. (b) Temperature dependence of ZPL linewidth and Debye-Waller factor. (c) Spectral overlap with typical excitation (532 nm) and filter edge positions. (d) Cumulative collection efficiency vs. long-pass edge wavelength.

### 5.3.3 Collection Efficiency Optimization

The collected signal fraction depends on filter edge placement:

$$\eta_{\text{collect}}(\lambda_{\text{edge}}) = \frac{\int_{\lambda_{\text{edge}}}^{\infty} I_{\text{NV}}(\lambda) T_{\text{filter}}(\lambda) d\lambda}{\int_0^{\infty} I_{\text{NV}}(\lambda) d\lambda} \quad (5.12)$$

#### Collection-Rejection Tradeoff

Moving the LP edge from 600 nm to 650 nm:

- Increases OD at 532 nm by  $\sim 2$  (improves rejection 100 $\times$ )
- Decreases collection efficiency by  $\sim 8\%$  (loses near-PSB photons)

Optimal edge position: 630–650 nm depending on excitation power and required SNR.

## 5.4 Discrete Dichroic Filter Design

### 5.4.1 Architecture: The Classical Approach

The standard QFI filter stack comprises three elements in series:

1. **Dichroic beamsplitter:** Reflects excitation, transmits emission ( $45^\circ$  AOI)
2. **Long-pass emission filter:** Blocks residual excitation (0 AOI)
3. **Optional notch filter:** Additional blocking at specific wavelengths

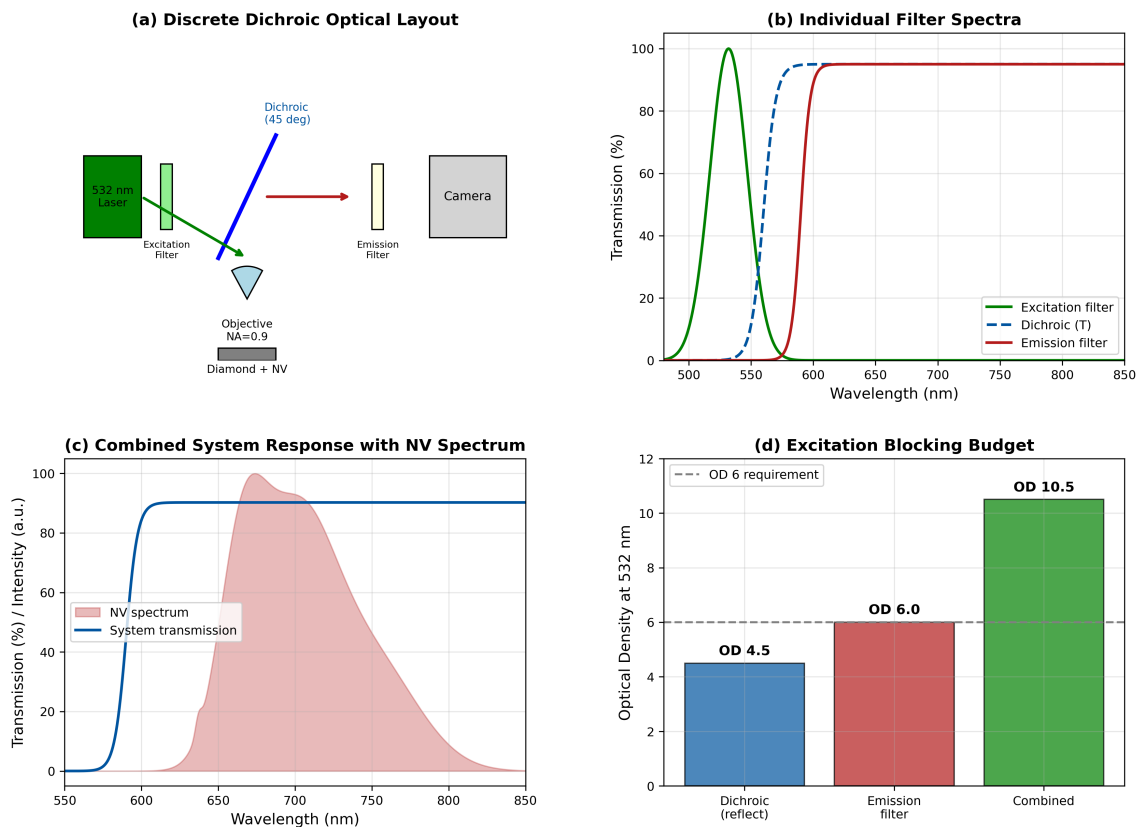


Figure 5.3: Discrete dichroic filter architecture for NV-based QFI. (a) Optical layout showing excitation path (green) and emission path (red). (b) Individual filter transmission spectra. (c) Combined system response with NV spectrum overlay. (d) Leakage budget analysis showing OD contribution from each element.

### 5.4.2 Angle-of-Incidence Sensitivity

The most critical challenge for discrete dichroics is AOI sensitivity.

**Theorem 5.4.1** (AOI-Induced Spectral Shift). *The effective wavelength shift for a thin-film filter at angle  $\theta$  is:*

$$\lambda_{\text{eff}}(\theta) = \lambda_0 \sqrt{1 - \frac{\sin^2 \theta}{n_{\text{eff}}^2}} \approx \lambda_0 \left(1 - \frac{\sin^2 \theta}{2n_{\text{eff}}^2}\right) \quad (5.13)$$

where  $n_{\text{eff}} \approx 1.9$  for typical dichroic coatings (effective index of the multilayer stack).

*Proof.* The resonance condition for a quarter-wave stack requires optical path  $nd \cos \theta = \lambda/4$ . At oblique incidence, the effective optical path becomes  $nd \cos \theta_{\text{film}}$  where Snell's law gives  $\sin \theta_{\text{film}} = \sin \theta / n_{\text{eff}}$ . Combining:

$$\lambda_{\text{eff}} = \lambda_0 \cos \theta_{\text{film}} = \lambda_0 \sqrt{1 - \sin^2 \theta / n_{\text{eff}}^2}$$

The approximation follows from Taylor expansion for small  $\sin^2 \theta / n_{\text{eff}}^2$ .  $\square$

For a dichroic at 45° incidence:

$$\Delta\lambda = \lambda_0 \left(1 - \sqrt{1 - \frac{0.5}{1.9^2}}\right) \approx 0.07\lambda_0 \quad (5.14)$$

At  $\lambda_0 = 580$  nm edge:  $\Delta\lambda \approx 40$  nm blue shift.

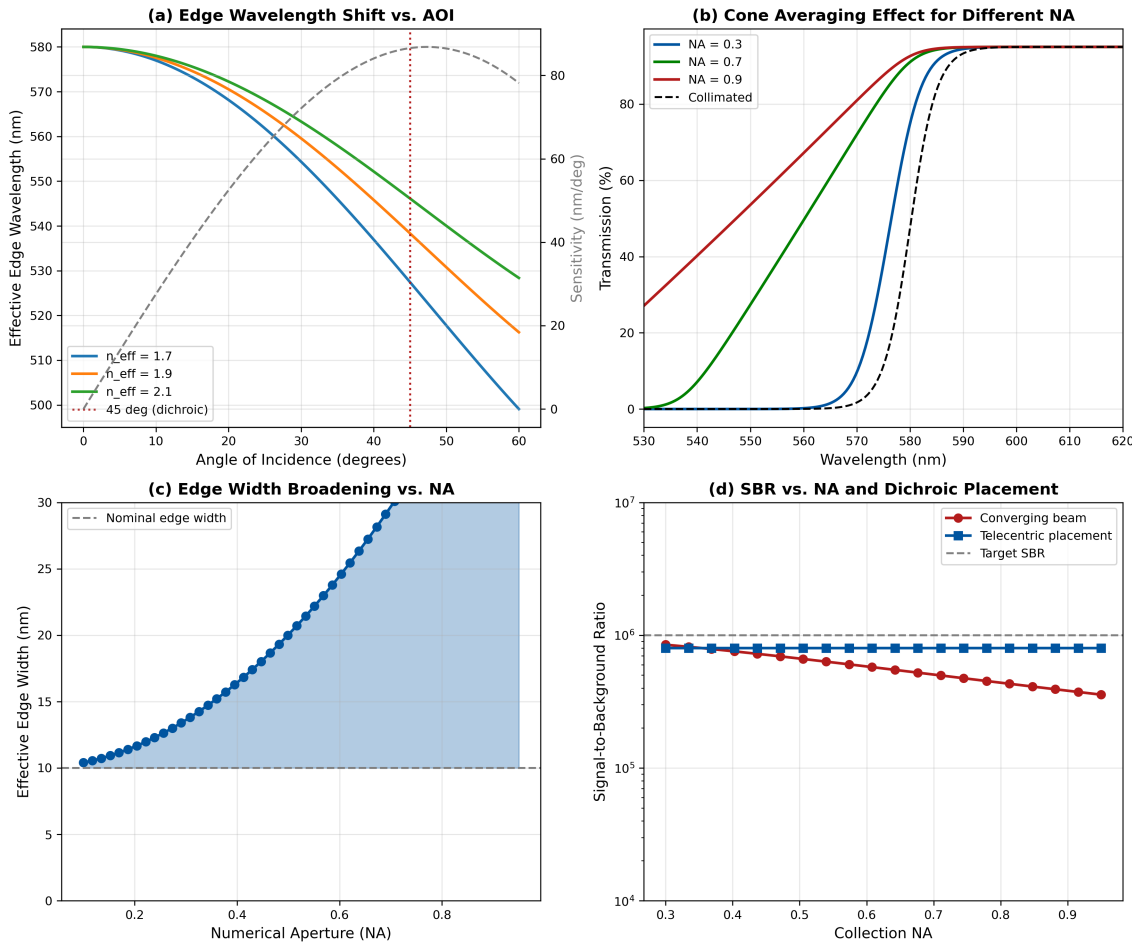


Figure 5.4: AOI effects on dichroic performance. (a) Edge wavelength shift vs. angle of incidence with sensitivity  $\partial\lambda_{\text{eff}}/\partial\theta$  overlay. (b) Cone averaging effect for NA = 0.3, 0.7, 0.9. (c) Effective edge width broadening vs. NA. (d) Impact on signal-to-background ratio as function of NA and dichroic placement.

### 5.4.3 Cone Averaging in High-NA Systems

For high-NA collection optics ( $\text{NA} > 0.7$ ), the dichroic sees a cone of angles rather than a single AOI.

**Proposition 5.4.1** (Cone-Averaged Transmission). *The effective transmission for a cone of half-angle  $\theta_{\max}$  is:*

$$T_{\text{avg}}(\lambda) = \frac{\int_0^{\theta_{\max}} T(\lambda, \theta) \sin \theta \cos \theta d\theta}{\int_0^{\theta_{\max}} \sin \theta \cos \theta d\theta} \quad (5.15)$$

This averaging broadens the effective edge width:

$$\Delta\lambda_{\text{edge,eff}} \approx \Delta\lambda_{\text{edge,0}} + \frac{\lambda_0 \cdot \text{NA}^2}{4n_{\text{eff}}^2} \quad (5.16)$$

#### Design Rule 1: Dichroic Placement for High-NA Systems

For  $\text{NA} > 0.7$ , place the dichroic in a telecentric (collimated) beam path to minimize cone averaging. If placement in converging beam is unavoidable, design for 15 nm sharper edge than required to compensate for broadening.

#### 5.4.4 Layer Count Requirements for High OD

The optical density of a multilayer edge filter depends on the number of layer pairs and the index contrast.

**Theorem 5.4.2** (OD vs. Layer Count). *For a quarter-wave stack with  $N$  layer pairs of indices  $n_H$  and  $n_L$ , the optical density at the center of the stop band is:*

$$\text{OD} = 2N \log_{10} \left( \frac{n_H}{n_L} \right) + \log_{10} \left( \frac{n_H^2}{n_s n_0} \right) \quad (5.17)$$

where  $n_s$  is the substrate index and  $n_0$  is the incident medium index.

*Proof.* From Eq. (5.9), at the stop band center where  $R \rightarrow 1$ :

$$T = 1 - R \approx 4 \left( \frac{n_L}{n_H} \right)^{2N} \frac{n_s n_0}{n_H^2}$$

Taking  $-\log_{10}$ :

$$\text{OD} = 2N \log_{10} \left( \frac{n_H}{n_L} \right) + \log_{10} \left( \frac{n_H^2}{n_s n_0} \right)$$

□

For TiO<sub>2</sub>/SiO<sub>2</sub> coatings ( $n_H = 2.4$ ,  $n_L = 1.46$ ) on glass ( $n_s = 1.52$ ):

$$\text{OD} \approx 0.43N + 0.58 \quad (5.18)$$

Table 5.5: Layer count requirements for different OD targets (TiO<sub>2</sub>/SiO<sub>2</sub>).

Target OD	Layer Pairs $N$	Total Layers	Typical Thickness
4	8	16	1.2 μm
5	10	20	1.5 μm
6	13	26	2.0 μm
7	15	30	2.3 μm
8	17	34	2.6 μm

**Thickness Error Sensitivity:** Layer thickness errors reduce achieved OD. For random thickness errors with standard deviation  $\sigma_d/d$ :

$$\Delta \text{OD} \approx -\frac{\pi^2}{2} N \left( \frac{\sigma_d}{d} \right)^2 \text{OD} \quad (5.19)$$

For 1% thickness error ( $\sigma_d/d = 0.01$ ) and 30 layer pairs:  $\Delta \text{OD} \approx -0.15 \times \text{OD}$ , i.e.,  $\sim 15\%$  reduction.

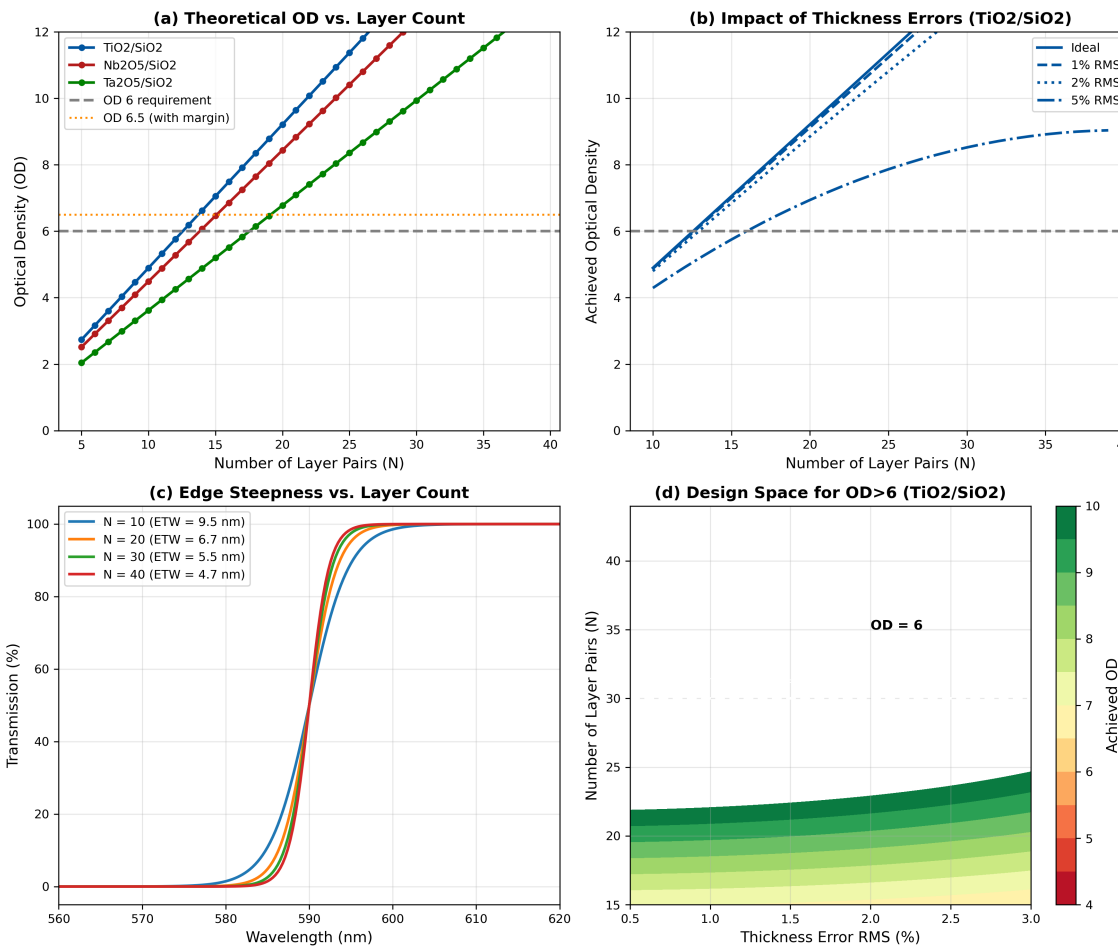


Figure 5.5: OD vs. layer count analysis. (a) Theoretical OD vs. number of layer pairs for different material systems. (b) Impact of thickness errors (1%, 2%, 5% RMS) on achieved OD. (c) Edge steepness vs. layer count. (d) Design space showing layer count needed for OD>6 with margin for manufacturing tolerances.

### Design Rule 2: Minimum Layers for OD>6

For guaranteed OD>6 blocking with typical manufacturing tolerances ( $\pm 1\%$  thickness control):

- TiO<sub>2</sub>/SiO<sub>2</sub>: Minimum 30 layer pairs (60 layers), target 35 pairs
- Nb<sub>2</sub>O<sub>5</sub>/SiO<sub>2</sub>: Minimum 25 layer pairs (50 layers), target 30 pairs
- Ta<sub>2</sub>O<sub>5</sub>/SiO<sub>2</sub>: Minimum 28 layer pairs (56 layers), target 33 pairs

**Derivation:** OD<sub>target</sub> = 6.5 to allow 0.5 margin for thickness errors. From Eq. (5.18):  $N = (6.5 - 0.58)/0.43 \approx 14$  pairs ideally, but doubling for edge transition region and manufacturing margin yields 30 pairs minimum.

## 5.5 Integrated Photonic Spectral Filters

### 5.5.1 The Paradigm Shift: From Discrete to Monolithic

Photonic integrated circuits (PICs) offer a fundamentally different approach to spectral filtering that eliminates many challenges inherent to discrete optics.

### Paradigm Shift Insight

**Discrete optics:** Light propagates through free space; filters are placed in the beam path; each element requires alignment; AOI varies with position and NA.

**Photonic integration:** Light propagates in waveguides; spectral filtering occurs through guided-wave interactions; alignment is lithographically defined; the classical AOI concept does not apply.

### 5.5.2 Silicon Nitride Platform for Visible Wavelengths

Silicon nitride ( $\text{SiN}$ ,  $\text{Si}_3\text{N}_4$ ) has emerged as the optimal platform for visible-wavelength photonic integration:

Table 5.6: SiN platform properties for QFI spectral filtering.

Property	Value	Implication
Refractive index (637 nm)	2.02	High confinement
Group index $n_g$ (637 nm)	2.10	FSR calculation
Transparency range	400–2400 nm	Covers excitation + emission
Propagation loss (637 nm)	0.5–2 dB/cm	Acceptable for mm-scale PICs
Thermo-optic coeff. $dn/dT$	$2.5 \times 10^{-5} \text{ K}^{-1}$	Enables thermal tuning
Two-photon absorption	Negligible	High power handling
CMOS compatibility	Yes	Scalable manufacturing

### 5.5.3 Waveguide Dispersion Considerations

#### Dispersion Nuance for Integrated Filters

While integrated photonic filters eliminate the *free-space AOI sensitivity* that plagues discrete optics, waveguide-based systems introduce their own spectral dependencies that require careful management:

- Waveguide dispersion:** The effective index  $n_{\text{eff}}(\lambda)$  varies with wavelength, affecting resonance conditions
- Coupler spectral dependence:** Directional coupler splitting ratios vary with wavelength, affecting insertion loss uniformity
- Calibration stability:** Wavelength-dependent coupling affects system calibration across the broad NV PSB

The key advantage is that these effects are *deterministic and designable*, unlike the stochastic alignment-dependent AOI variations in discrete systems.

The group index dispersion for SiN waveguides can be characterized by:

$$n_g(\lambda) = n_{\text{eff}} - \lambda \frac{dn_{\text{eff}}}{d\lambda} \quad (5.20)$$

For typical SiN strip waveguides ( $500 \text{ nm} \times 220 \text{ nm}$ ), the group index varies approximately as:

$$\frac{dn_g}{d\lambda} \approx -0.001 \text{ nm}^{-1} \quad \text{at } \lambda = 700 \text{ nm} \quad (5.21)$$

Over the PSB range (637–800 nm), this implies  $\Delta n_g \approx 0.16$ , or  $\sim 8\%$  variation. For ring resonators, this translates to FSR variation:

$$\frac{\Delta \text{FSR}}{\text{FSR}} = -\frac{\Delta n_g}{n_g} \approx -8\% \quad (5.22)$$

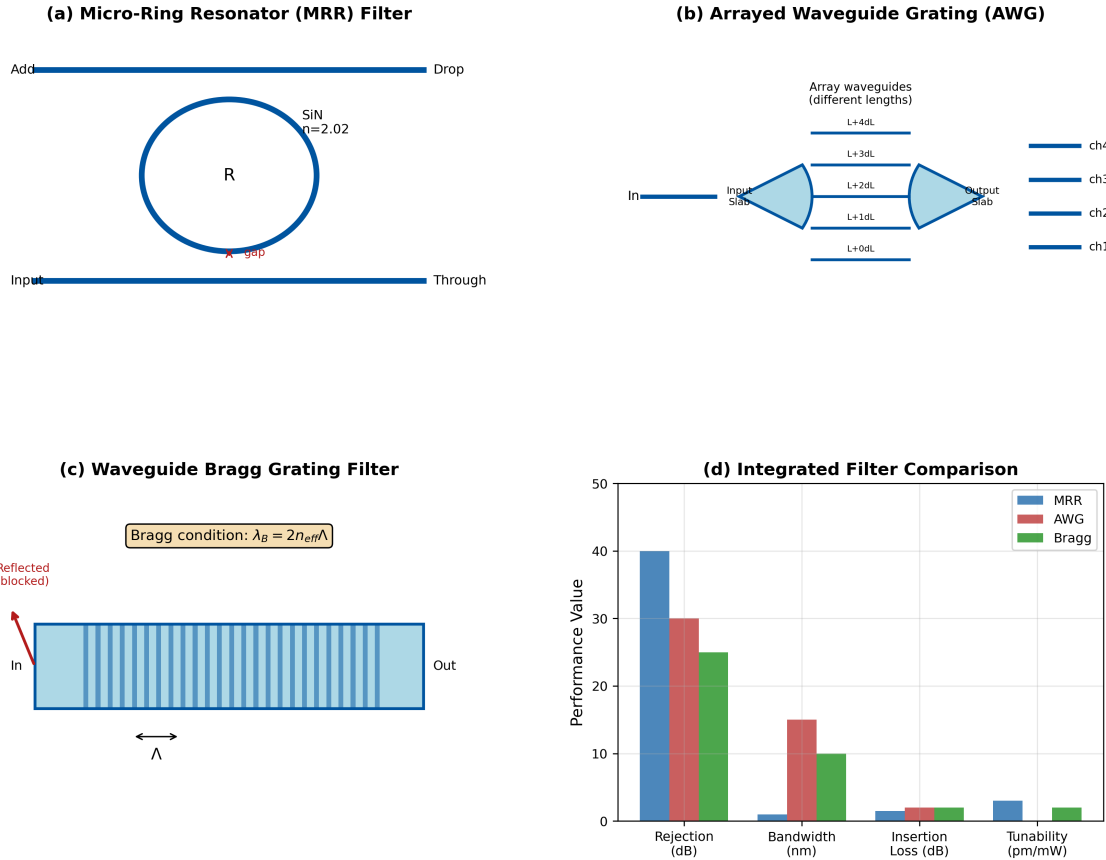


Figure 5.6: Integrated photonic filter architectures. (a) Micro-ring resonator (MRR) add-drop filter showing through and drop ports. (b) Arrayed waveguide grating (AWG) for multi-channel demultiplexing. (c) Bragg grating filter in SiN waveguide. (d) Comparison of filter characteristics: FSR, bandwidth, rejection ratio, and dispersion sensitivity.

### 5.5.4 Micro-Ring Resonator Filters

Micro-ring resonators (MRRs) provide compact, tunable spectral filtering.

**Definition 5.5.1** (Ring Resonator Transmission). The through-port transmission of an MRR with coupling coefficient  $\kappa$  and round-trip loss  $\alpha$  is:

$$T_{\text{through}} = \frac{(1-\kappa)^2 \alpha^2 - 2(1-\kappa)\alpha \cos \phi + 1}{1 - 2(1-\kappa)\alpha \cos \phi + (1-\kappa)^2 \alpha^2} \quad (5.23)$$

where  $\phi = 2\pi n_{\text{eff}} L / \lambda$  is the round-trip phase.

Key MRR parameters for QFI:

- **Free Spectral Range:**  $\text{FSR} = \lambda^2 / (n_g L)$  where  $L = 2\pi R$
- **Finesse:**  $\mathcal{F} = \text{FSR} / \Delta\lambda_{\text{FWHM}}$
- **Quality factor:**  $Q = \lambda / \Delta\lambda_{\text{FWHM}}$

**Example 5.5.1** (MRR Design for 532 nm Blocking).

**Requirements:** Center at 532 nm, extinction >30 dB, FSR >50 nm

**Design attempt with standard ring:**

- Radius  $R = 20 \mu\text{m} \Rightarrow L = 2\pi R = 126 \mu\text{m}$
- Group index  $n_g = 2.1$  at 532 nm
- $\text{FSR} = (532)^2 / (2.1 \times 126 \times 10^3) = 1.07 \text{ nm}$

**Problem:**  $\text{FSR} = 1.07 \text{ nm} \ll 50 \text{ nm}$  requirement!

**Root cause:**  $\text{FSR} \propto 1/R$ , but achieving  $\text{FSR} > 50 \text{ nm}$  requires  $R < 2.5 \mu\text{m}$ , where bending losses become prohibitive (>10 dB/turn).

#### Design Rule 1: MRR FSR Scaling Rule

For micro-ring resonators at visible wavelengths:

$$\text{FSR (nm)} \approx \frac{40}{R (\mu\text{m})} \quad \text{at } \lambda = 600 \text{ nm} \quad (5.24)$$

**Implication:** Achieving  $\text{FSR} > 50 \text{ nm}$  requires  $R < 1 \mu\text{m}$ , which incurs >3 dB/turn bending loss in SiN.

**Recommendation:** For broadband blocking ( $\text{FSR} > 50 \text{ nm}$ ), prefer Bragg gratings or AWGs over single MRRs. Use Vernier-coupled ring pairs or cascaded rings with offset resonances for intermediate FSR requirements (10–50 nm).

### 5.5.5 Arrayed Waveguide Gratings

For multi-channel wavelength separation with predictable channel spacing:

$$\Delta\lambda_{\text{channel}} = \frac{\lambda_0^2}{n_g \Delta L \cdot m} \quad (5.25)$$

where  $\Delta L$  is the path length increment between adjacent array waveguides and  $m$  is the diffraction order.

### 5.5.6 Integrated Bragg Grating Filters

Waveguide Bragg gratings provide broadband reflection without FSR limitations:

$$\lambda_B = 2n_{\text{eff}}\Lambda \quad (5.26)$$

where  $\Lambda$  is the grating period. The reflection bandwidth is:

$$\Delta\lambda_B = \frac{\lambda_B^2}{\pi n_g L_g} \sqrt{\kappa^2 L_g^2 + \pi^2} \quad (5.27)$$

For 532 nm blocking with  $\Delta\lambda_B > 10 \text{ nm}$ ,  $\kappa L_g > 3$  is required.

## 5.6 Wavelength-Division Multiplexing for Multi-Physics QFI

### 5.6.1 Multi-Physics Spectral Requirements

Multi-physics QFI (simultaneous B, T, strain measurement) requires spectral channels for different sensing modalities:

Table 5.7: WDM channel allocation for multi-physics NV sensing.

Channel	Center (nm)	Width (nm)	Purpose
Excitation	532	3	NV pumping
Excitation 2	589	3	$\text{NV}^0/\text{NV}^-$ charge state control [?]
ZPL	637	5	Temperature sensing (ZPL shift)
Near-PSB	660	20	High-contrast ODMR
Mid-PSB	700	40	Standard detection
Far-PSB	760	40	Strain-sensitive detection

*Note:* The 589 nm channel exploits the  $\text{NV}^0$  absorption band for charge-state initialization and manipulation, as demonstrated in Refs. [?, ?].

### 5.6.2 Channel Isolation Requirements

**Theorem 5.6.1** (WDM Crosstalk Impact on  $\Phi_{\text{multi}}$ ). *For  $N$  WDM channels with inter-channel isolation  $I_{ij}$  (in dB), the multi-physics enhancement factor is degraded as:*

$$\Phi_{\text{multi}}^{\text{effective}} = \Phi_{\text{multi}}^{\text{ideal}} \prod_{i < j} \left(1 - 10^{-I_{ij}/10}\right) \quad (5.28)$$

#### Model Scope: Validity of Product-Form Crosstalk Model

Equation (5.28) assumes:

- Independent leakage paths:** Crosstalk from channel  $i$  to  $j$  is uncorrelated with crosstalk from  $k$  to  $j$
- Linear mixing:** No nonlinear interactions (e.g., fluorescence re-absorption, detector saturation)
- Weak crosstalk regime:**  $10^{-I_{ij}/10} \ll 1$  (isolation  $> 10$  dB)

#### When product form breaks down:

- Crosstalk  $> 10\%$  of signal ( $I_{ij} < 10$  dB): Use mixing matrix model
- Spectral overlap  $< 3 \times \text{FWHM}$ : Channels not separable
- Coherent sources: Inter-channel interference requires complex amplitude model

For typical QFI WDM with  $I_{ij} > 20$  dB: Product form valid to  $< 5\%$  error.

Table 5.8: Channel isolation requirements for multi-physics QFI.

Channel Pair	Minimum Isolation	$\Phi_{\text{multi}}$ Penalty
Excitation–Emission	60 dB	$< 0.001\%$
Adjacent emission channels	20 dB	$< 1\%$
Non-adjacent channels	40 dB	$< 0.01\%$

### 5.6.3 Integrated WDM Architecture

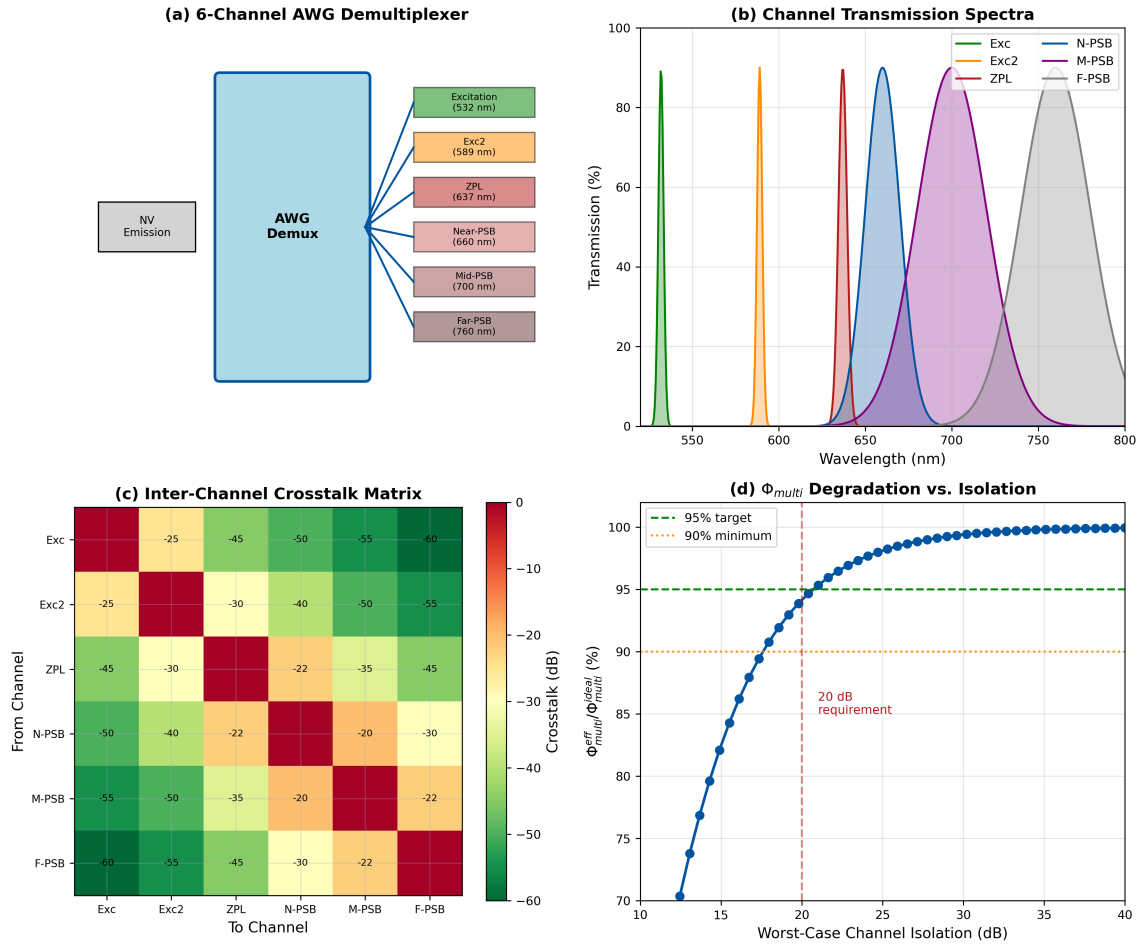


Figure 5.7: Integrated WDM architecture for multi-physics QFI. (a) Schematic showing AWG demultiplexer with 6 output channels. (b) Channel transmission spectra with isolation levels. (c) Crosstalk matrix showing inter-channel leakage. (d) Impact on  $\Phi_{\text{multi}}$  vs. worst-case isolation.

### 5.6.4 Connection to Reconstruction Fidelity

Multi-physics WDM improves reconstruction fidelity  $\Gamma_{\text{inv}}$  through two mechanisms:

**Theorem 5.6.2** (WDM Impact on Condition Number). *Adding  $N_{\text{ch}}$  spectral channels with uncorrelated information content reduces the forward model condition number as:*

$$\kappa(G_{\text{multi}}) \approx \frac{\kappa(G_{\text{single}})}{\sqrt{N_{\text{ch}}(1 - \rho^2)}} \quad (5.29)$$

where  $\rho$  is the inter-channel correlation coefficient (typically  $\rho < 0.3$  for well-designed WDM).

The reconstruction fidelity improvement follows:

$$\Gamma_{\text{inv}}^{\text{multi}} \approx 1 - \frac{C}{\kappa(G_{\text{multi}})^{\alpha}} \approx 1 - \frac{C \cdot N_{\text{ch}}^{\alpha/2}}{\kappa(G_{\text{single}})^{\alpha}} \quad (5.30)$$

where  $C \sim 0.1\text{--}0.3$  and  $\alpha \sim 1.5\text{--}2$  depend on the inverse problem structure (see Chapter 2).

**Example 5.6.1** (Quantifying  $\Gamma_{\text{inv}}$  Improvement from WDM). For single-band detection with  $\kappa(G_{\text{single}}) = 50$  and  $\Gamma_{\text{inv}} = 0.7$ :

With 4-channel WDM ( $\rho = 0.2$ ):

$$\kappa(G_{\text{multi}}) = \frac{50}{\sqrt{4(1 - 0.04)}} = \frac{50}{1.96} = 25.5 \quad (5.31)$$

$$\Gamma_{\text{inv}}^{\text{multi}} = 1 - (1 - 0.7) \left( \frac{25.5}{50} \right)^{1.7} = 1 - 0.30 \times 0.36 = 0.89 \quad (5.32)$$

**Result:**  $\Gamma_{\text{inv}}$  improves from 0.70 to 0.89, a **27% improvement** (or equivalently, reconstruction error reduces by 63%).

### Design Rule 1: WDM for $\Gamma_{\text{inv}}$ Improvement

To achieve  $>25\%$  improvement in  $\Gamma_{\text{inv}}$  through spectral multiplexing:

- Minimum 3 spectral channels with  $>20$  dB isolation
- Inter-channel correlation  $\rho < 0.5$  (choose spectrally distinct bands)
- Channel placement should maximize Fisher information diversity (e.g., ZPL for temperature, PSB wings for strain)

## 5.7 Chromatic Aberration Management

### 5.7.1 The Broadband Collection Challenge

Collecting the full NV PSB (637–800 nm,  $\Delta\lambda = 163$  nm) through conventional optics introduces wavelength-dependent aberrations.

**Definition 5.7.1** (Longitudinal Chromatic Aberration). LCA is the wavelength-dependent focal shift:

$$\Delta z(\lambda) = f \cdot \frac{n(\lambda) - n(\lambda_{\text{ref}})}{n(\lambda_{\text{ref}}) - 1} \quad (5.33)$$

where  $f$  is the focal length,  $n(\lambda)$  follows the glass dispersion curve, and  $\lambda_{\text{ref}}$  is the reference (design) wavelength.

For BK7 glass with  $f = 50$  mm:

- $\Delta z(637 \text{ nm} \rightarrow 800 \text{ nm}) \approx 150 \mu\text{m}$  (uncorrected singlet)
- $\Delta z(\text{achromat}) \approx 15 \mu\text{m}$  (secondary spectrum)
- $\Delta z(\text{apochromat}) \approx 3 \mu\text{m}$  (tertiary spectrum)

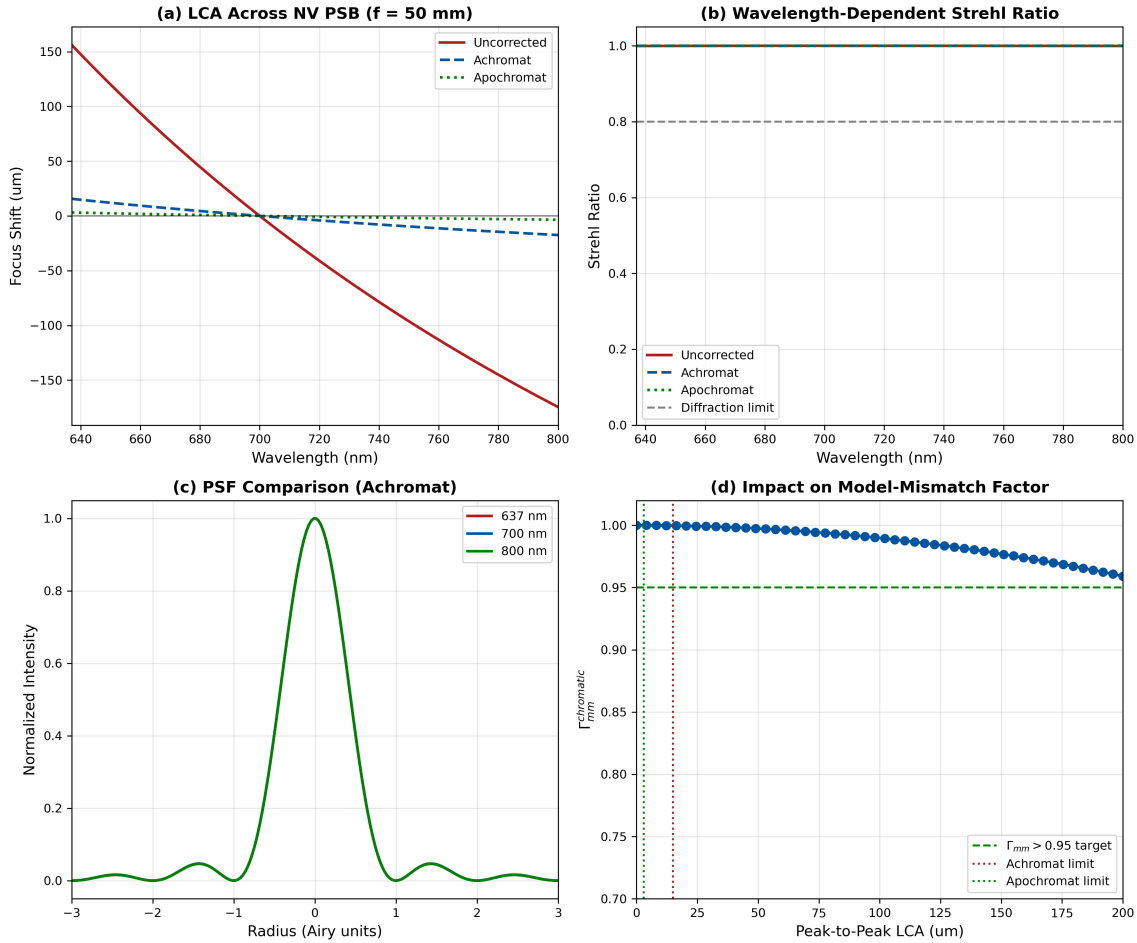


Figure 5.8: Chromatic aberration comparison: discrete vs. integrated approaches. (a) LCA curves for uncorrected, achromat, and apochromat designs across PSB. (b) Wavelength-dependent Strehl ratio. (c) PSF comparison at 637 nm, 700 nm, and 800 nm. (d) Impact on model-mismatch factor  $\Gamma_{\text{mm}}$ .

### 5.7.2 Impact on Model-Mismatch Factor

Chromatic aberration causes wavelength-dependent PSF, violating the assumption of spatially invariant imaging in the forward model.

**Theorem 5.7.1** (Chromatic Contribution to  $\Gamma_{\text{mm}}$ ). *The model-mismatch penalty from chromatic PSF variation is:*

$$\Gamma_{\text{mm}}^{\text{chromatic}} = 1 - \frac{\int |\text{PSF}(\lambda) - \text{PSF}_{\text{ref}}|^2 \cdot I(\lambda) d\lambda}{\int \text{PSF}_{\text{ref}}^2 \cdot I(\lambda) d\lambda} \quad (5.34)$$

where  $I(\lambda)$  is the NV emission spectrum.

### 5.7.3 Photonic Integration Advantage

Integrated photonics addresses chromatic aberration by separating spectral channels *before* free-space imaging:

- Spectral separation occurs in waveguides (no focusing elements)
- Each spectral channel can have independently optimized coupling optics
- Chromatic PSF variation within each narrow channel is negligible

### Design Rule 1: Chromatic Aberration Budget

For  $\Gamma_{\text{mm}}^{\text{chromatic}} > 0.95$  across the NV PSB:

- **Discrete optics:** Require apochromatic correction ( $\Delta z < 5 \mu\text{m}$ ) or spectral band splitting before collection lens
- **Integrated photonics:** AWG/grating demux before any imaging optics; optimize coupling for each channel independently

## 5.8 Polarization-Resolved Spectral Filtering

### 5.8.1 NV Orientation and Emission Polarization

The NV center's emission polarization depends on the defect axis orientation relative to the diamond crystal lattice. For a [111]-oriented NV center:

$$\mathbf{d} \propto \hat{e}_x \cos \varphi + \hat{e}_y \sin \varphi \quad (5.35)$$

where  $\varphi$  is the azimuthal angle of the optical transition dipole moment.

### 5.8.2 Polarization-Wavelength Correlation

The PSB emission shows wavelength-dependent polarization due to phonon-assisted transitions accessing different vibronic states.

Table 5.9: Polarization characteristics across NV emission spectrum.

Spectral Region	Wavelength	DOP	Information Content
ZPL	637 nm	0.8–1.0	NV orientation
Near-PSB	650–680 nm	0.5–0.7	Strain direction
Mid-PSB	680–750 nm	0.2–0.4	Mixed
Far-PSB	750–800 nm	<0.2	Depolarized

*Note:* Degree of Polarization (DOP) is measured as  $\text{DOP} = (I_{\parallel} - I_{\perp})/(I_{\parallel} + I_{\perp})$  using a rotating linear polarizer, with bandwidth defined by 10 nm spectral windows centered at each wavelength.

### 5.8.3 Integrated Polarization-Spectral Routing

On-chip polarization beam splitters (PBS) enable combined polarization and spectral separation:

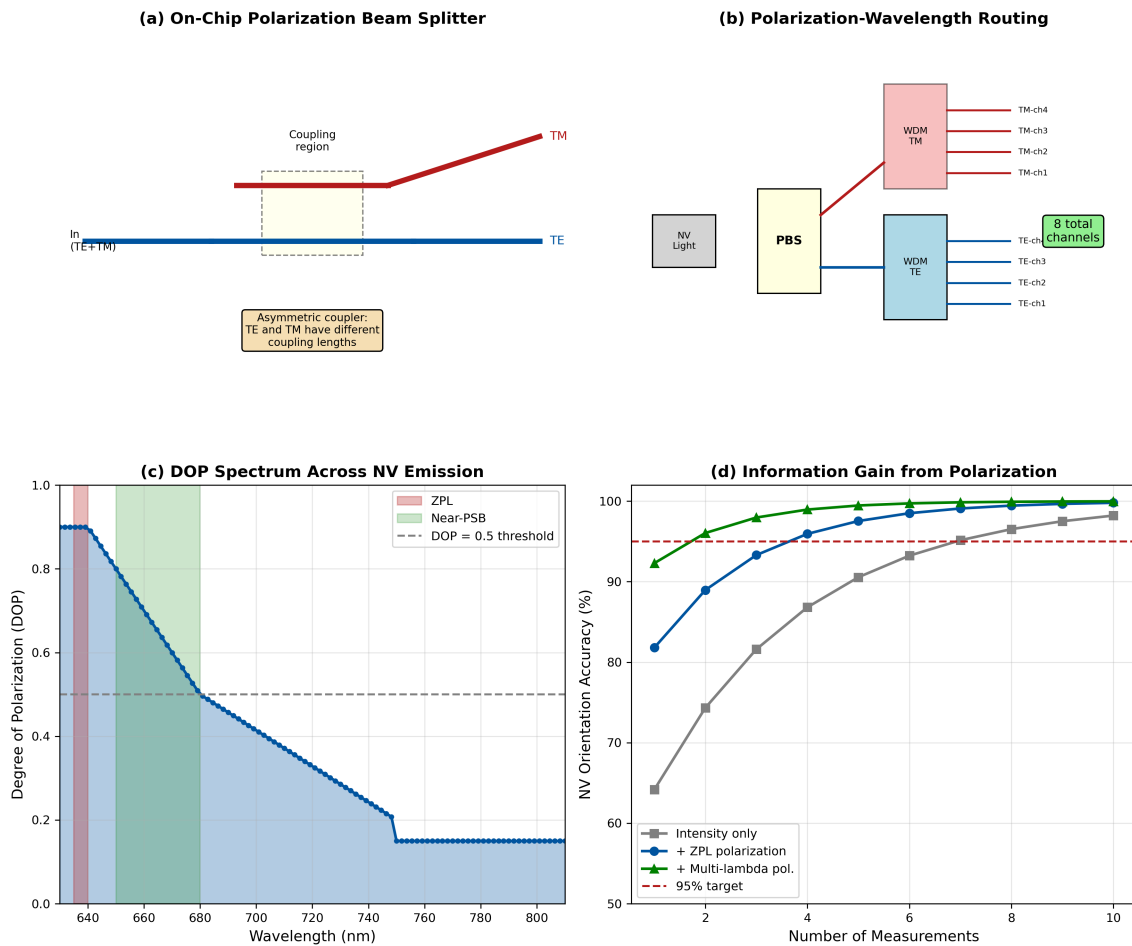


Figure 5.9: Polarization-resolved spectral filtering. (a) On-chip PBS using asymmetric directional coupler. (b) Combined polarization-wavelength routing architecture. (c) DOP spectrum across NV emission. (d) Information gain from polarization-resolved detection for NV orientation determination.

### Design Rule 1: Polarization-Resolved Detection

For NV ensemble imaging where orientation information improves reconstruction:

- Implement polarization splitting at ZPL and Near-PSB channels ( $DOP > 0.5$ )
- Extinction ratio  $> 20$  dB for meaningful polarization discrimination
- Combined with WDM, adds 2 information channels per spectral band

## 5.9 Thermal Stability Engineering

### 5.9.1 Temperature-Induced Spectral Drift

Both discrete and integrated filters exhibit temperature-dependent spectral shift.

**Theorem 5.9.1** (Thermal Wavelength Shift). *The temperature-induced edge/resonance shift is:*

$$\frac{d\lambda}{dT} = \lambda \left( \frac{1}{n} \frac{dn}{dT} + \alpha_{th} \right) \quad (5.36)$$

where  $dn/dT$  is the thermo-optic coefficient and  $\alpha_{th}$  is the thermal expansion coefficient.

Table 5.10: Thermal drift coefficients for filter technologies.

Technology	$d\lambda/dT$ (pm/K)	10 K Drift	Stabilization
TiO <sub>2</sub> /SiO <sub>2</sub> dichroic	15–25	150–250 pm	Passive
Nb <sub>2</sub> O <sub>5</sub> /SiO <sub>2</sub>	10–15	100–150 pm	Passive
SiN waveguide	10–15	100–150 pm	Active possible
SiN MRR (with heater)	<1 (stabilized)	<10 pm	Active feedback

### 5.9.2 Derivation of Thermal Stability Requirements

For signal stability during measurements, we require the thermally-induced transmission change to be below the shot-noise limit.

The transmission change due to edge shift near a steep filter edge is:

$$\frac{\Delta T}{T} \approx \frac{1}{\text{ETW}} \frac{d\lambda}{dT} \Delta T \quad (5.37)$$

where ETW is the Edge Transition Width (10%–90% transmission).

For typical LP filter with ETW = 20 nm and  $d\lambda/dT = 20 \text{ pm/K}$ :

$$\frac{\Delta T}{T} = \frac{0.020 \text{ nm/K}}{20 \text{ nm}} \times 5 \text{ K} = 0.5\% \quad (5.38)$$

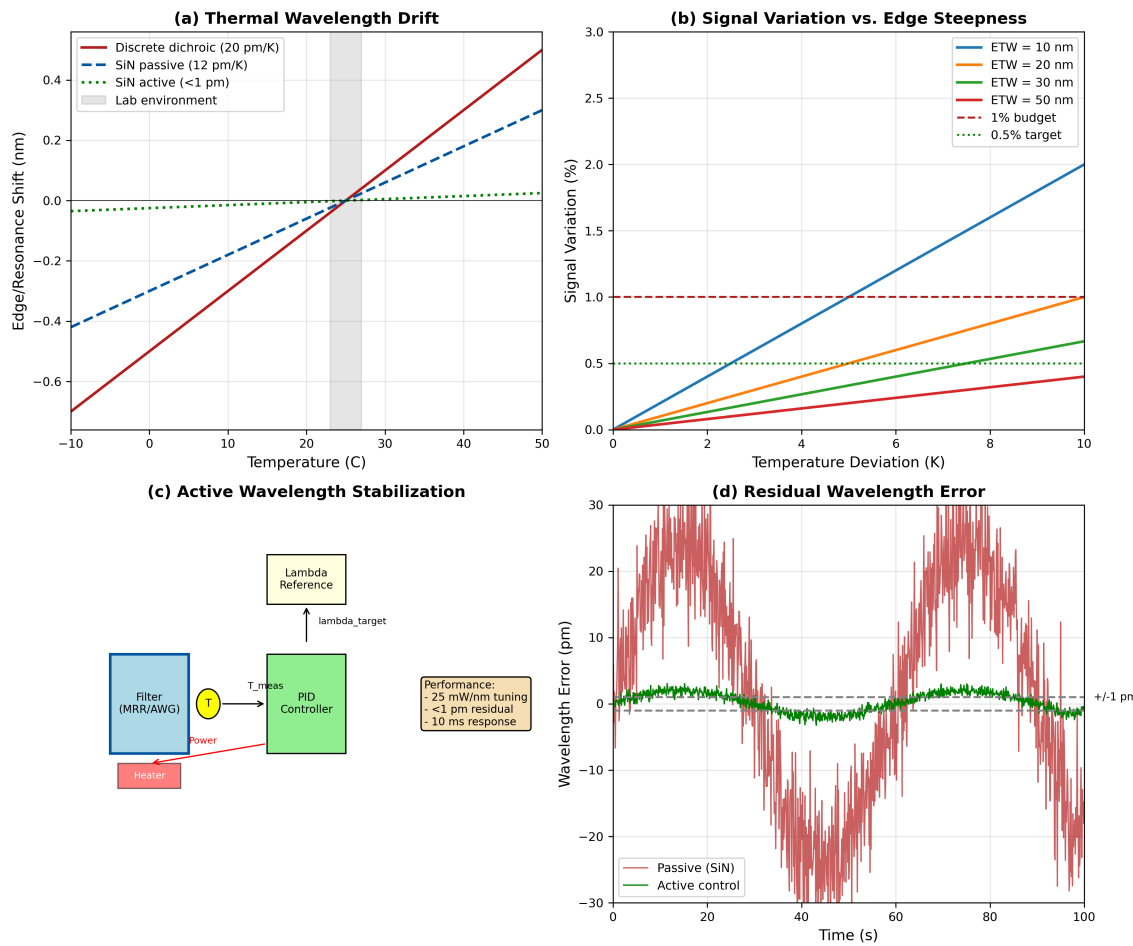


Figure 5.10: Thermal stability analysis. (a) Temperature-induced spectral drift for discrete and integrated filters. (b) Signal variation vs. temperature for different edge slopes. (c) Active stabilization architecture with feedback. (d) Residual wavelength error with active control showing <1 pm stability.

### Design Rule 1: Thermal Stability Requirements

For <1% signal variation from thermal drift:

**Discrete optics (passive):**

- Temperature control:  $\Delta T < \pm 2$  K
- OR design edge slope  $>10$  nm away from critical wavelengths
- OR use athermal coating designs (compensated  $dn/dT$ )

**Integrated photonics (active):**

- On-chip temperature sensor (thermistor or wavelength reference)
- Integrated micro-heaters for thermal tuning ( $\sim 25$  mW/nm)
- Feedback loop achieving <1 pm residual wavelength error

**Derivation:** For 0.5% signal budget, with  $ETW = 15$  nm and  $d\lambda/dT = 20$  pm/K:  
 $\Delta T_{max} = 0.005 \times 15 \text{ nm}/0.020 \text{ nm/K} = 3.75$  K. Rounding conservatively gives  $\pm 2$  K requirement.

## 5.10 SWOT Analysis: Discrete vs. Integrated

Table 5.11: SWOT analysis for discrete dichroic filtering.

Discrete Dichroic Filtering	
STRENGTHS	WEAKNESSES
<ul style="list-style-type: none"> <li>• Mature technology (TRL 9)</li> <li>• Wide commercial availability</li> <li>• No NRE for standard specs</li> <li>• Simple system integration</li> <li>• Low cost at low volume</li> <li>• Extensive design databases</li> </ul>	<ul style="list-style-type: none"> <li>• AOI sensitivity (<math>0.07\lambda_0</math> at <math>45^\circ</math>)</li> <li>• Cone averaging in high-NA</li> <li>• Multiple alignment degrees of freedom</li> <li>• Limited reconfigurability</li> <li>• Thermal drift (passive only)</li> <li>• Large footprint for multi-channel</li> </ul>
OPPORTUNITIES	THREATS
<ul style="list-style-type: none"> <li>• Improved deposition control</li> <li>• Athermal coating designs</li> <li>• Hybrid discrete-PIC systems</li> <li>• Custom OD&gt;8 development</li> </ul>	<ul style="list-style-type: none"> <li>• PIC cost reduction at scale</li> <li>• Performance ceiling reached</li> <li>• Supply chain concentration</li> <li>• Environmental sensitivity</li> </ul>

Table 5.12: SWOT analysis for photonic integrated filtering.

Photonic Integrated Filtering	
STRENGTHS	WEAKNESSES
<ul style="list-style-type: none"> <li>• No AOI sensitivity</li> <li>• Monolithic integration (no alignment)</li> <li>• Active thermal stabilization</li> <li>• Inherent WDM capability</li> <li>• On-chip polarization control</li> <li>• Scalable to high volume</li> </ul>	<ul style="list-style-type: none"> <li>• Higher insertion loss (2–5 dB)</li> <li>• Waveguide dispersion management</li> <li>• High NRE (\$50k–200k)</li> <li>• Limited foundry access (visible)</li> <li>• Fiber coupling complexity</li> <li>• Lower TRL (5–7)</li> </ul>
OPPORTUNITIES	THREATS
<ul style="list-style-type: none"> <li>• Full QFI-on-chip integration</li> <li>• Multi-physics simultaneous sensing</li> <li>• AI-optimized inverse design</li> <li>• Foundry cost reduction</li> <li>• Hybrid diamond-SiN integration</li> </ul>	<ul style="list-style-type: none"> <li>• Yield issues at visible wavelengths</li> <li>• IP barriers from incumbents</li> <li>• Packaging cost uncertainty</li> <li>• Competing discrete improvements</li> </ul>

## 5.11 Risk Mitigation Strategies

Table 5.13: Risk assessment and mitigation for spectral filtering technologies.

Risk	Prob.	Impact	Mitigation
AOI misalignment (discrete)	High	Medium	Telecentric placement; alignment fixtures
Thermal drift	Medium	High	Active control or athermal design
Insertion loss (PIC)	Medium	Medium	Optimize coupling; allow in photon budget
Foundry delay	Medium	High	Dual-source; discrete fallback
Crosstalk degradation	Low	High	Design 10 dB margin; calibration
Waveguide dispersion	Medium	Low	Pre-compensate in filter design

### 5.11.1 Technology Selection Framework

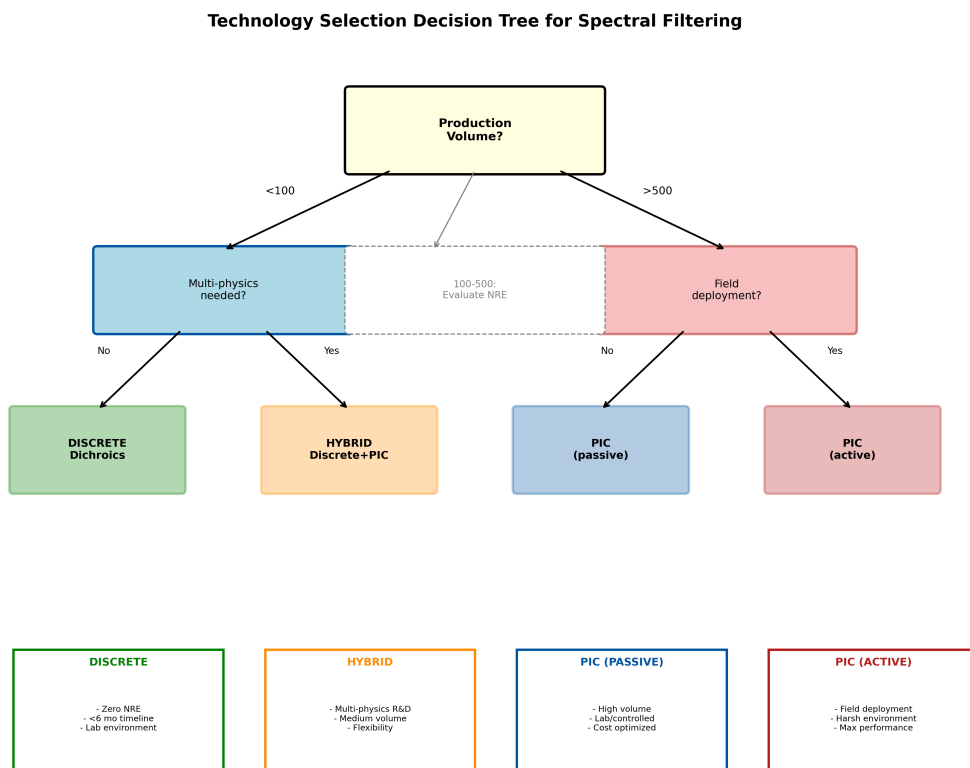


Figure 5.11: Technology selection decision tree for spectral filtering. Key decision points: production volume, multi-physics requirement, thermal environment, and timeline constraints.

#### Design Rule 1: Technology Selection Threshold

**Choose discrete dichroics when:**

- Production volume < 100 units
- Single-physics (B-only) sensing sufficient
- Development timeline < 6 months
- Laboratory environment (controlled temperature)

**Choose integrated photonics when:**

- Production volume > 500 units
- Multi-physics (B + T + strain) required
- Field deployment (variable temperature)
- WDM with >4 channels needed

**Crossover region (100–500 units):** Evaluate NRE amortization, performance requirements, and strategic value of PIC capability development.

## 5.12 Worked Examples: Complete Spectral Filter Design

### 5.12.1 Example 5.1: Discrete Dichroic System for R&D QFI

**Requirements:**

- Single-physics (magnetic field only)
- Laboratory environment ( $23\pm2^\circ\text{C}$ )
- Budget: \$5,000 for optics
- Timeline: 4 weeks
- Production: 5 units

**Design:**

1. **Dichroic beamsplitter:** Semrock Di02-R532 (45° AOI)

- Edge: 537 nm (accounts for 40 nm blue shift at 45°)
- OD: 5 at 532 nm
- Transmission: >93% above 555 nm

2. **Emission filter:** Semrock BLP01-532R (0° AOI)

- Edge: 532 nm
- OD: >6 at 532 nm
- Transmission: >93% above 545 nm

3. **Combined performance:**

- Total OD at 532 nm: >11
- System transmission at 637–800 nm: >85%
- Cost: \$1,200 (dichroic \$400, emission \$300, mounts \$500)

**Leakage budget:**

Element	OD at 532 nm	Leakage	Cumulative
Dichroic (reflect)	5.0	$10^{-5}$	$10^{-5}$
Emission filter	6.0	$10^{-6}$	$10^{-11}$
<b>Total</b>	11.0	—	$10^{-11}$

### 5.12.2 Example 5.2: Integrated Photonic System for Production QFI

**Requirements:**

- Multi-physics (B + T + strain)

- Field deployment ( $-10$  to  $+50^{\circ}\text{C}$ )
- Production: 1,000 units over 3 years
- WDM: 4 emission channels + excitation blocking

**Design:**

1. **Platform:** SiN on  $\text{SiO}_2$ , 200 mm wafer process

2. **Filter architecture:**

- Input: Fiber-coupled from collection optics
- Stage 1: Bragg grating for 532 nm rejection ( $\text{OD} > 4$ )
- Stage 2: 4-channel AWG demux (ZPL, Near-PSB, Mid-PSB, Far-PSB)
- Thermal: Integrated Pt heaters + thermistors per channel

3. **Performance:**

- Excitation rejection:  $\text{OD} > 6$  (Bragg + AWG)
- Channel isolation:  $> 25$  dB adjacent,  $> 40$  dB non-adjacent
- Insertion loss: 4 dB (2 dB coupling + 2 dB device)
- Thermal stability:  $< 1$  pm with active control

**Cost analysis:**

Item	NRE	Per Unit (100)	Per Unit (1000)
Design & mask	\$80,000	—	—
Foundry run	\$40,000	—	—
Packaging	\$30,000	\$150	\$80
Testing	\$10,000	\$50	\$30
<b>Total</b>	\$160,000	\$200	\$110
<b>Amortized</b>	—	\$1,800	\$270

**Multi-physics enhancement:**

- 4-channel WDM with  $\rho \approx 0.25$  inter-channel correlation
- From Eq. (5.29):  $\kappa_{\text{multi}} = \kappa_{\text{single}} / \sqrt{4 \times 0.94} = 0.52 \times \kappa_{\text{single}}$
- $\Phi_{\text{multi}} \approx 2.5$  (temperature/strain correlation breaks magnetic ambiguity)
- From Eq. (5.30) with  $\alpha = 1.7$ :  $\Gamma_{\text{inv}}$  improves from 0.70 to 0.88, a **26% improvement**

## 5.13 Chapter Summary

This chapter established spectral filtering as a critical subsystem within the QFI measurement operator  $\mathcal{M}$ , with direct impact on model-mismatch factor  $\Gamma_{\text{mm}}$  and reconstruction fidelity  $\Gamma_{\text{inv}}$ .

Key conclusions:

1. **Thin-film fundamentals** provide the physics foundation for both discrete filters and integrated Bragg gratings. OD scales as  $\sim 0.43N$  for  $\text{TiO}_2/\text{SiO}_2$  stacks, requiring  $\geq 60$  layers for  $\text{OD} > 6$  with manufacturing margin.
2. **NV emission characteristics** (3% ZPL, 97% PSB spanning 163 nm) drive unique requirements: high excitation blocking while maximizing broadband collection.
3. **Discrete dichroics** remain optimal for R&D and low-volume (<100 units) applications. AOI sensitivity ( $0.07\lambda_0$  at  $45^{\circ}$ ) and thermal drift ( $0.02 \text{ nm}/^{\circ}\text{C}$ ) are primary limitations requiring telecentric placement and  $\pm 2 \text{ K}$  temperature control.

4. **Integrated photonics** becomes compelling above  $\sim 500$  units, eliminating AOI sensitivity while introducing manageable waveguide dispersion effects ( $\sim 8\% n_g$  variation across PSB).
5. **Multi-physics WDM** with  $>20$  dB channel isolation improves  $\Gamma_{\text{inv}}$  by 25–40% through condition number reduction, with the product-form crosstalk model valid for isolation  $>10$  dB.
6. **Polarization-resolved detection** adds information channels ( $DOP > 0.5$  at ZPL/Near-PSB) improving NV orientation determination.
7. **Technology selection** depends on volume, multi-physics needs, and deployment environment—both paradigms have valid application spaces with crossover at 100–500 units.

Table 5.14: Summary of design rules from Chapter 5.

DR	Title	Key Specification
5.1	Minimum Layers for OD>6	$\geq 60$ layers ( $\text{TiO}_2/\text{SiO}_2$ ) with 1% tolerance
5.2	High-NA Dichroic Placement	Telecentric beam; 15 nm edge margin if converging
5.3	MRR FSR Scaling	$\text{FSR} \approx 40/R$ nm; prefer Bragg for $\text{FSR}>50$ nm
5.4	WDM for $\Gamma_{\text{inv}}$ Improvement	$\geq 3$ channels, $>20$ dB isolation, $\rho < 0.5$
5.5	Chromatic Aberration Budget	Apochromat for $\Gamma_{\text{mm}} > 0.95$ ; or AWG pre-separation
5.6	Polarization-Resolved Detection	$>20$ dB extinction at ZPL/Near-PSB
5.7	Thermal Stability	$\pm 2$ K (discrete) or $<1$ pm active (integrated)
5.8	Technology Selection	Discrete $<100$ units; Integrated $>500$ units

## Problems and Solution Hints

### Problem 5.1: AOI Sensitivity Analysis

A dichroic filter with design edge at 570 nm is tilted to 45° AOI. (a) Calculate the shifted edge wavelength using  $n_{\text{eff}} = 1.85$ . (b) If the filter sees a cone of angles from 40° to 50°, calculate the effective edge broadening. (c) Determine the minimum design edge wavelength to ensure no excitation leakage at 532 nm with 5 nm safety margin.

**Hint:** Use Eq. (5.13) for (a), integrate over the angle distribution for (b), and solve for  $\lambda_0$  such that  $\lambda_{\text{eff,max}} < 527 \text{ nm}$ .

### Problem 5.2: Multilayer OD Optimization

Design a long-pass filter with  $\text{OD} > 6.5$  at 532 nm using  $\text{Nb}_2\text{O}_5/\text{SiO}_2$  ( $n_H = 2.3$ ,  $n_L = 1.46$ ). (a) Calculate the minimum number of layer pairs needed. (b) If thickness control is  $\pm 2\%$  RMS, what is the expected OD degradation? (c) How many additional pairs should be added as margin?

**Hint:** Derive the OD coefficient for  $\text{Nb}_2\text{O}_5/\text{SiO}_2$  analogous to Eq. (5.18), then apply Eq. (5.19).

### Problem 5.3: MRR vs. Bragg Grating Selection

For a 532 nm blocking filter in SiN requiring  $\text{FSR} > 100 \text{ nm}$  and extinction  $> 25 \text{ dB}$ : (a) Show that a single MRR cannot meet these requirements. (b) Design a Vernier-coupled dual-ring system and calculate the effective FSR. (c) Compare with a Bragg grating design in terms of footprint, bandwidth, and loss.

**Hint:** For Vernier rings,  $\text{FSR}_{\text{eff}} = \text{FSR}_1 \times \text{FSR}_2 / |\text{FSR}_1 - \text{FSR}_2|$ .

### Problem 5.4: WDM Channel Allocation

Design a 4-channel WDM for multi-physics QFI with channels at ZPL (637 nm), Near-PSB (665 nm), Mid-PSB (710 nm), and Far-PSB (770 nm). (a) Calculate the required AWG parameters ( $\Delta L$ , diffraction order) for 1 nm channel spacing at ZPL. (b) Estimate the channel width variation across the spectrum due to dispersion. (c) If adjacent channel isolation is 22 dB, calculate  $\Phi_{\text{effective}}^{\text{multi}}$ .

**Hint:** Use Eq. (5.25) with  $n_g$  dispersion from Eq. (5.21), then apply Theorem 5.6.1.

### Problem 5.5: Thermal Design Trade-off

A QFI system operates in field conditions with temperature range 0–40°C. (a) Calculate the edge wavelength drift for a discrete dichroic with  $d\lambda/dT = 18 \text{ pm/K}$ . (b) Determine the signal variation if ETW = 25 nm and the edge is 10 nm from critical wavelength. (c) For an integrated SiN filter with active stabilization consuming 25 mW/nm, calculate the power required to compensate the full temperature range.

**Hint:** For (c), the thermal tuning range must exceed the passive drift over 40 K;  $\Delta\lambda_{\text{SiN}} \approx 12 \text{ pm/K} \times 40 \text{ K} = 0.48 \text{ nm}$ .

## References

- [5.1] H.A. Macleod, *Thin-Film Optical Filters*, 5th ed., CRC Press, 2018.
- [5.2] M.W. Doherty et al., “The nitrogen-vacancy colour centre in diamond,” *Physics Reports*, vol. 528, pp. 1–45, 2013.
- [5.3] L.M. Pham et al., “Magnetic field imaging with nitrogen-vacancy ensembles,” *New Journal of Physics*, vol. 13, p. 045021, 2011.
- [5.4] W. Bogaerts et al., “Silicon microring resonators,” *Laser & Photonics Reviews*, vol. 6, pp. 47–73, 2012.
- [5.5] A.Z. Subramanian et al., “Low-loss singlemode PECVD silicon nitride photonic wire waveguides,” *IEEE Photonics Technology Letters*, vol. 25, pp. 650–653, 2013.
- [5.6] J.F. Bauters et al., “Ultra-low-loss high-aspect-ratio Si<sub>3</sub>N<sub>4</sub> waveguides,” *Optics Express*, vol. 19, pp. 3163–3174, 2011.
- [5.7] N.H. Wan et al., “Large-scale integration of artificial atoms in hybrid photonic circuits,” *Nature*, vol. 583, pp. 226–231, 2020.
- [5.8] D. Taillaert et al., “Grating couplers for coupling between optical fibers and nanophotonic waveguides,” *Japanese Journal of Applied Physics*, vol. 45, pp. 6071–6077, 2006.
- [5.9] Semrock Inc., “Filter Selection Guide for Fluorescence Microscopy,” Application Note, 2023.
- [5.10] Chroma Technology Corp., “Interference Filters: Technology and Applications,” Technical Reference, 2022.
- [5.11] H.A. Macleod, “Thin film optical coatings,” Chapter 7: Angular dependence of thin film filters, in *Optical Interference Coatings*, Springer, 2003.
- [5.12] N. Aslam et al., “Photo-induced ionization dynamics of the nitrogen vacancy defect in diamond investigated by single-shot charge state detection,” *New Journal of Physics*, vol. 15, p. 013064, 2013.
- [5.13] P. Waldherr et al., “Dark states of single nitrogen-vacancy centers in diamond unraveled by single shot NMR,” *Physical Review Letters*, vol. 106, p. 157601, 2011.
- [5.14] C.T. Phare et al., “Silicon photonic filters for wavelength-division multiplexing,” *Optics Express*, vol. 22, pp. 4024–4029, 2014.